# Calculation of three-phase bubble columns

Dierk Wiemann<sup>a</sup>, Dieter Mewes

Institute of Process Engineering, University of Hannover, Hannover, Germany a present: Bayer Technology Services GmbH, Uerdingen, Germany

#### **Abstract**

The scope of this work is the numerical calculation of the three-dimensional, time-dependent velocity and concentration fields in cylindrical bubble columns with two-phase gas-liquid and three-phase gas-liquid-solid flow. Therefore all phases are described by an Eulerian approach. In particular the local interfacial area density and the interphase transfer terms for mass and momentum are calculated based on a population balance equation approach. The proposed approach enables an effective way to couple population balance and computational fluid dynamics. For three-phase gas-liquid-solid flow heavy particles with diameters in the range of 100  $\mu$ m are considered as catalyst for a heterogeneous chemical reaction. The solids phase viscosity and pressure are described based on the granular flow theory. The influence of particles on bubble coalescence has been investigated to extend the model. From the calculation the three-dimensional, time-dependent velocity and concentration fields are obtained.

**Keywords**: bubble column, population balance equation, CFD, mass transfer,

# 1. Introduction

The flow pattern in bubble columns is strongly influenced by the superficial gas velocity. The homogeneous flow regime arises for low superficial gas velocities. In this flow regime the integrated volume fraction of gas and the interfacial area density increase almost linearly with the superficial gas velocity. However for technical applications the heterogeneous flow regime is of more importance. In this flow regime increasing coalescence of small bubbles lead to the formation of larger ones. These large bubbles rise up much faster than the small ones thus a large amount of gas is entrapped with them. The liquid flow pattern is characterized by large scale vortices, which cause a large degree of backmixing. If mass transfer occurs between the gas and the liquid phase backmixing influences the local concentration difference.

The dimension of bubble column reactors is widely based on empirical models for the interfacial area, the phase velocities and backmixing (Deckwer [1], Nigam and Schumpe [2]). The scale-up of these models is however limited to the experimental dimensions since the reactor geometry has a strong influence on these parameters. In contrast computational fluid dynamic methods enable a physical based prediction of the flow field independent of the column dimension. For the description of bubbly flow the Euler-multi-fluid model and the Euler-Lagrange approach are commonly used for the calculation of large-scale flow fields. Other approaches such as direct numerical simulations are restricted to detailed investigations of small numbers of bubbles.

The description of bubbly flow requires the knowledge of the interfacial area since mass, momentum and energy transport are proportional to it. Therefore the population balance equation is often used to calculate the interfacial area in dependence of the flow field. In this work the multi-fluid model is coupled with a population balance equation

approach according to Lehr et al. [3]. From the numerical solution of the population balance equation a bi-modal bubble size distribution is obtained for the heterogeneous flow regime, thus the gas phase can be divided into one fraction containing small bubbles and a second fraction containing large bubbles. Using the self-similarity of the calculated bubble size distributions a transport equation for the mean bubble diameter of the small and large bubble fraction is derived. Both bubble fractions are coupled by bubble coalescence and break-up, thus the volume fraction and the bubble size vary throughout the flow field.

# 2. Modeling bubbly flow

In this section the model is described briefly. A detailed description can be found in [4] to [6].

The calculation considers three Eulerian phases: the liquid phase, a gas phase representing small bubbles and a gas phase representing large bubbles. For three phase gas-liquid-solid flow an additional Eulerian phase arises for the solid phase. For each phase the momentum transport equation

$$\begin{split} \frac{\partial}{\partial t} \left( \alpha_{i} \rho_{i} \vec{u}_{i} \right) + \nabla \left( \alpha_{i} \left( \rho_{i} \vec{u}_{i} \vec{u}_{i} \right) \right) = \\ -\alpha_{i} \nabla p_{i} + \nabla \left( \alpha_{i} \eta_{i} \left( \Delta \vec{u}_{i} + \left( \Delta \vec{u}_{i} \right)^{T} \right) \right) + \vec{F}_{mass} + \alpha_{i} \rho_{i} \vec{g} + \vec{F}_{ij} \end{split}, \quad i = g_{1}, g_{2}, 1 \quad (1)$$

is solved independent of the physical phase distribution. The inIn the above equation all phases share the same bulk pressure. The temporal and convective changes of momentum on the left hand side of eq. (1) are balanced by several forces on the right hand side. These forces are due to the bulk pressure gradient, shear, secondary fluxes due to mass transfer, gravitational forces and interphase momentum transfer. The index I refers to the liquid phase,  $g_1$  and  $g_2$  refer to the small and the large bubble phase. For the multi-fluid approach in particular modeling of the interphase momentum transfer is important. The most important interphase force is due to interphase drag. The drag force per unit volume is calculated to

$$\vec{F}_{il} = C_D \frac{3}{4} \rho_l \frac{\alpha_i}{d_i} |\vec{u}_i - \vec{u}_l| (\vec{u}_i - \vec{u}_l).$$
 (2)

based on the drag on a single sphere. In eq. (2) the drag coefficient is calculated following Clift et al. [7]

$$C_{D} = \max \left[ \frac{24}{Re} (1 + 0.1 Re^{0.75}); \min \left\{ \max(0.44, \frac{2}{3} Eo^{1/2}), \frac{8}{3} \right\} \right]$$
 (3)

in dependence of the Reynolds- and Eotvos-number

$$Re_i = \frac{|\vec{u}_i - \vec{u}_1|d_i}{v_1} \tag{4}$$

$$Eo = \frac{g(\rho_1 - \rho_i)d_i^2}{\sigma}.$$
 (5)

In eq. (5) the surface tension between the liquid and gas phase is  $\sigma$ . The Sauter-bubble diameter  $d_i$  is calculated from a transport equation for the mean bubble volume (Lehr et al. [3]). In addition secondary fluxes of momentum occur due to mass flux between the phases

$$\vec{F}_{mass} = \begin{cases} -\dot{M}_{i \to j} \vec{u}_i, & \text{phase i} \\ \dot{M}_{i \to j} \vec{u}_i, & \text{phase j} \end{cases}$$
 (6)

In eq.(5) the mass flux from phase i to phase j is labeled  $\dot{M}_{i\to j}$ . For the gas phase also secondary fluxes due to coalescence and break-up of bubbles are considered. The bulk mass balance equation for each phase is

$$\frac{\partial(\alpha_{i}\rho_{i})}{\partial t} + \nabla(\alpha_{i}\rho_{i}\vec{u}_{i}) = \begin{cases}
-\dot{M}_{i\rightarrow 1}, i = 1,2 \\
+\dot{M}_{j\rightarrow 1}, i = 1; j = 1,2
\end{cases}$$
(7)

considering mass transfer from the gaseous to the liquid phase.

For multi-component flow with n species in addition to the bulk mass balance a species mass balance equation

$$\frac{\partial(\alpha_{i}\zeta_{Ai}\rho_{i})}{\partial t} + \nabla(\alpha_{i}\zeta_{Ai}\rho_{i}\vec{u}_{i}) - \nabla(D_{Ai}\nabla(\rho_{i}\zeta_{Ai})) = \begin{cases} -\zeta_{Ai}\dot{M}_{i\rightarrow 1}, i=1,2\\ +\zeta_{Ai}\dot{M}_{i\rightarrow 1}, i=1; j=1,2 \end{cases}$$
(8)

is solved for (n-1) species. In eq. (8) one of these (n-1) species is named A. The species represent the tracer substance or the transferring component. For the calculation of the mass transfer rate the phase equilibrium at the gas-liquid interface is described following Henry's law. The mass transfer across a turbulent air-water surface is investigated by Law and Khoo [8]. The experimental results indicate that the mass transfer rate is correlated to the turbulence near the surface. However the authors emphasize that for the implementation into a multi-fluid model the dependency between the near surface turbulence and the bulk phase turbulence needs further investigations. Therefore in this work the mass transfer coefficient is calculated in dependence of a Sherwood-number. The mass transfer rate is calculated

$$\dot{m}_{i,l} = \frac{c_1}{c_1 - c_{A,l}} \beta_l \left( \rho_{A,pl} - \rho_{A,l} \right)$$
 (9)

with the bulk molar concentration of the liquid phase  $c_l$  and the bulk molar concentration of the transferred component  $c_{A,l}$ . The Sherwood-number is calculated according to Brauer [12].

In bubbly flow turbulent velocity fluctuations arise in the liquid phase. These fluctuations are caused due to the shear flow but also the presence of the bubbles induce turbulence. So far no general accepted model for the description of the turbulence exists. In this work the turbulence in the liquid is described by the k-ε model with additional source terms accounting for bubble induced turbulence following the proposal of Lopez de Bertodano et al. [9].

For three-phase flow the solids phase is considered by an Eulerian-phase. The momentum balance is written to

$$\frac{\partial}{\partial t} (\alpha_{s} \rho_{s} \vec{u}_{s}) + \nabla (\alpha_{s} \rho_{s} \vec{u}_{s} \vec{u}_{s}) = -\alpha_{s} \nabla p - \nabla p_{s} + \nabla \left( \overline{\alpha_{s} \tau_{s}} \right) - \vec{F}_{d} + \rho_{s} \vec{g} . \tag{10}$$

In addition to the bulk pressure p the solids pressure  $p_s$  arises. The solids pressure describes the additional pressure due to interactions between the solids. Inter-particle collisions are considered by the shear stress tensor  $\tau$ . For the calculation of the solids pressure and the shear stress tensor the theory of granular flow is applied [10].

Collisions between solids and bubbles lead to momentum transfer between the gas and solid phases. Based on the assumption of elastic collisions the momentum transfer term

$$F_{d,g,s} = 3,519\alpha_i \alpha_s \rho_s \frac{1}{d_{Bi} + \frac{\rho_i}{\rho_s} \left(\frac{d_P}{d_{Bi}}\right)^2 d_P} u_{rel}^2$$
(11)

arises in the gas and solid phases. In eq. (11) the solids diameter is  $d_p$ , the diameter of the bubble is  $d_{Bi}$  and the relative velocity between solids and bubbles is  $u_{rel}$ .

For the description of the local bubble size and the local interfacial area density a simplified solution of the population balance equation is used. This model enables the prediction of the volume fraction and bubble size for homogeneous and heterogeneous bubbly flow. The resulting transport equations for the volume fraction and bubble size are coupled with the balance equation for mass and momentum. Thus the flow field is calculated in dependence of the local bubble size. In this work three-phase gas-liquid-flow with small but heavy particles is considered. The solids represent the catalyst for a heterogeneous chemical reaction.

The resulting set of equations is solved with the code CFX-5.7 using the method of finite volumes. The flow domain is discretized using a block-structured grid with hexahedral volumes. The edge length of the grid is 1 cm. Near the wall region a finer grid is used. The flow field in bubble columns strongly varies with time and space. For the temporal resolution time steps in the order of 0.01s to 0.05s are made. These time steps provide the calculation of the large-scale velocity fluctuations in the flow field. The convective terms are discretized with second order accuracy to reduce numerical diffusion.

#### 3. Results

# 3.1. Experimental investigation of coalescence in three-phase flow

The transport equation for the mean bubble volume describes the local bubble diameter in dependence of bubble-break-up and coalescence processes. For the case of small particles in the order of 100µm the collision between particles and bubbles does not cause bubble break-up. However bubble coalescence can be affected by the presence of solids. From two-phase gas-liquid flow it is known, that coalescence arises if the relative velocity between the bubbles perpendicular to their surface is smaller than a certain critical velocity. To determine the influence of solids loading on this critical velocity binary collisions between bubbles are analyzed.

The liquid phase is de-ionized water, the gas phase is air and the solids are glass spheres with a mean diameter of 78.11µm. In <u>fig. 1</u> several sequences for different solids loadings are depicted. From these images the relative velocity perpendicular to the bubbles surfaces is determined. For high velocities the bubbles bounce, whereas for small values coalescence occurs.

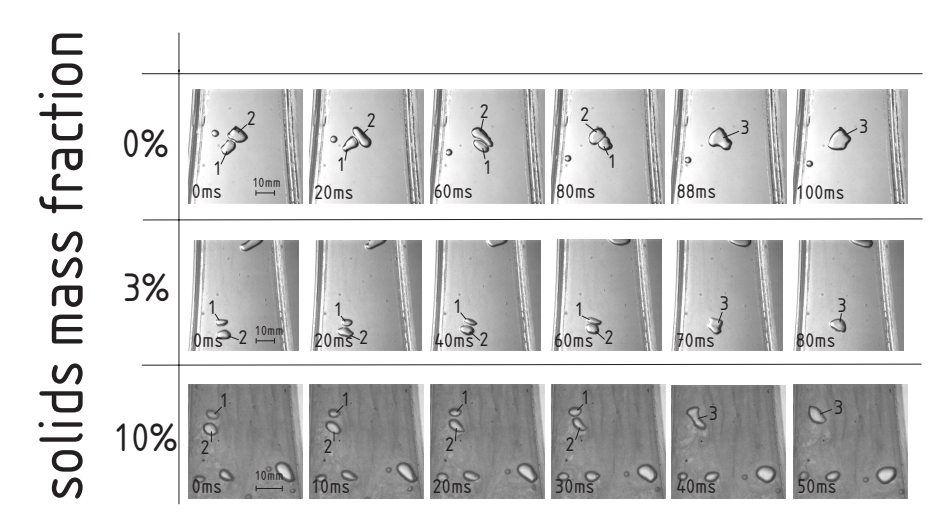


Figure 1: Bubble coalescence due to binary collisions for different solids loadings

In <u>fig. 2</u> the critical velocity is shown in dependence of the solids mass fraction. For two-phase gas-liquid flow the critical velocity is 0.095 m/s. In case of ten per cent solids mass fraction the critical velocity decreases to 0.06 m/s. Thus coalescence is hindered due to the presence of the glass spheres.

#### 3.2. Numerical calculated flow fields

From the numerical calculation the three-dimensional, time-dependent flow fields are obtained. The liquid is water, the gas phase is air. For the solid phase glass spheres of 100µm diameter are assumed. The overall solids loading is 0.114. In <u>fig.3</u> the instantaneous flow fields of the solid and liquid phase are shown. The streamlines of the

solid and the liquid phase are colored with the volume fraction and the axial velocity. The solids motion is similar to the liquids, thus the solids are transported upwards in the core region of the column and transported downwards near the column wall. In contrast to the volume fraction of gas, high volume fractions of solids are calculated near the wall, whereas low volume fractions are calculated in the core region.

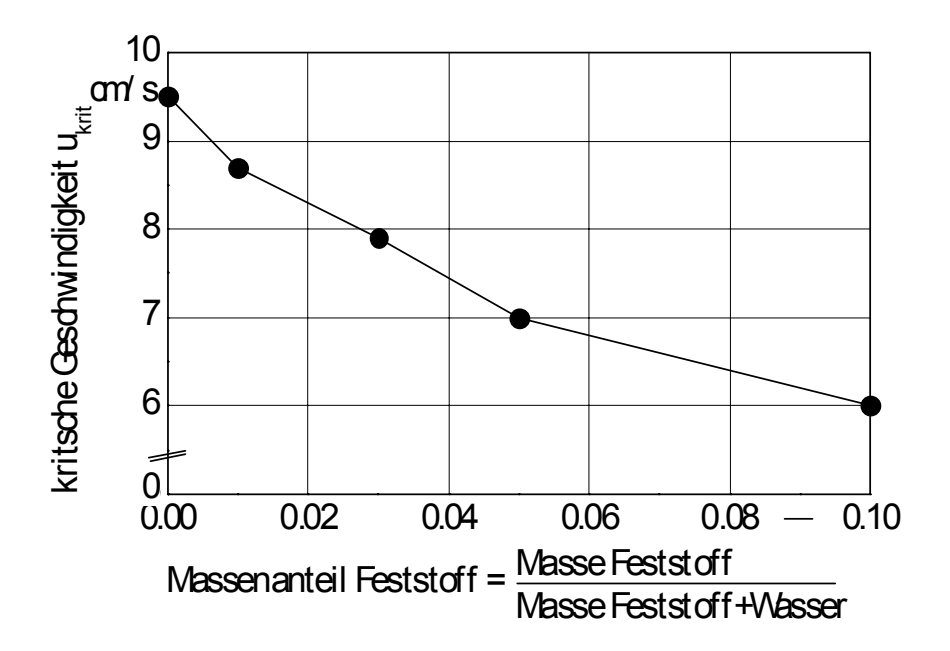


Figure 2: Influence of solids loading on the critical velocity

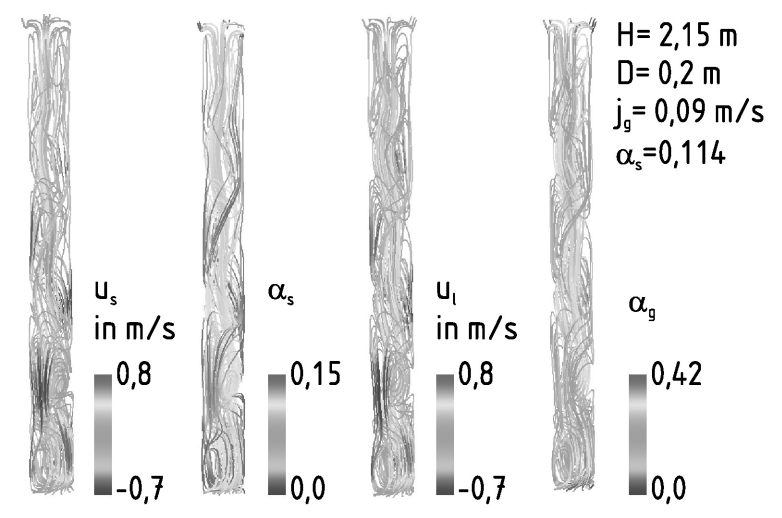


Figure 3: Calculated instantaneous flow field in a three-phase bubble column

The model is extended to consider a heterogenous chemical reaction for which the solids represent the catalyst. As example the hydrogenation of anthraquinone has been chosen. For that purpose the gas phase is assumed as hydrogen, the liquid is a solution, which contains a certain amount of anthraquinone. The solid particles represent the palladium catalyst. The model includes the absorption of the gas phase, the transport of the absorbed hydrogen and the anthraquinone to the solids surface and the chemical reaction at the surface. For the Euler model the chemical reaction is represented by a quasi-homogeneous reaction rate. The reaction rate depends on the volume fraction of solids, the solids density and the molar concentration of anthraquinone in the liquid phase. The chemical reaction rate is calculated to

$$\dot{\mathbf{r}}_{v} = \mathbf{k}_{r} \alpha_{s} \rho_{s} \mathbf{c}_{Anthr} \eta_{s} \tag{12}$$

In eq. (12) the constant is  $k_r$ =0.0014 m³/(kg s) [11] and the solids efficiency is set to  $\eta_s$ =1. The reaction rate is introduced in the mass balance equation thus an additional source term arises for the liquid phase, whereas for the gaseous phases sink terms arise. In fig. 4 the calculated volume fraction of the gas phase and the mass fractions of the absorbed hydrogen, the anthraquinone and the resulting hydroanthraquinone are shown. In accordance with the decrease of anthraquinone the mass fraction of hydroanthraquinone increases along the column height.

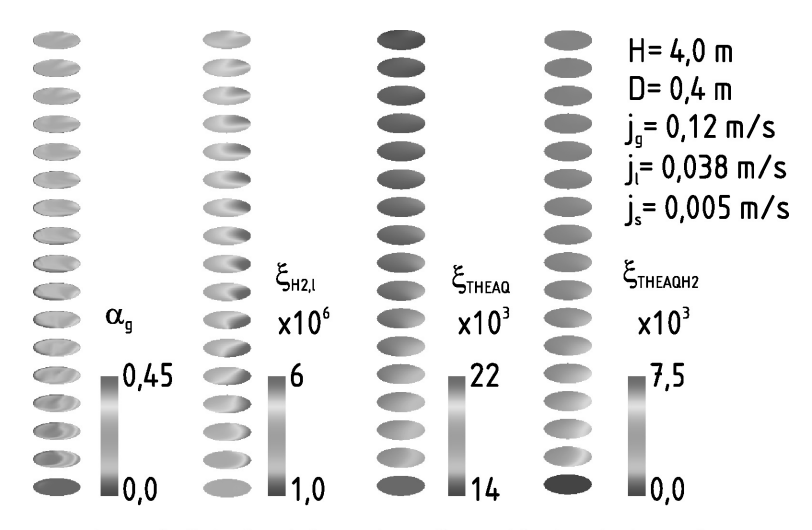


Figure 4: Calculated three-phase flow with chemical reaction

# 4. Conclusion

The three-dimensional, time-dependent flow fields for three-phase gas-liquid-solid flow in cylindrical bubble columns are calculated using an Eulerian model. In particular the balance equations for mass and momentum are coupled with a transport equation for the mean bubble volume. For a heterogeneous chemical reaction the solid phase is

considered as catalyst. The calculated flow fields are similar to those calculated for twophase gas-liquid flow.

## **Notation**

```
interfacial area density, m<sup>-1</sup>
              drag coefficient,
C_{D}
              molar concentration, mol m<sup>-3</sup>
c
D
              column diameter, m
d
              bubble diameter, m
              force, kg m s<sup>-2</sup>
F
              gravitational acceleration, m<sup>2</sup> s<sup>-1</sup>
g
Η
              Henry- coefficient, kg m<sup>-1</sup> s
              superficial velocity, m s<sup>-1</sup>
              turbulent kinetic energy per unit mass, m<sup>2</sup> s<sup>-2</sup>
k
              mass flux density, kg m<sup>-2</sup> s<sup>-1</sup>
m
              mass flux from phase i to j, kg m<sup>-3</sup> s<sup>-1</sup>
              molar flux density, mol m<sup>-2</sup> s<sup>-1</sup>
'n
              pressure, kg m<sup>-1</sup> s<sup>-2</sup>
p
              time, s
t
              velocity, m s-1
              coordinate, m
Greek letters
```

- α volume fraction,
- β mass transfer coefficient, m s<sup>-1</sup>
- ε turbulent kinetic energy dissipation rate, m<sup>2</sup> s<sup>-3</sup>
- η dynamic viscosity, kg m<sup>-1</sup> s<sup>-1</sup>
- μ molecular weight, kg mol<sup>-1</sup>
- ρ density, kg m<sup>-1</sup>
- v kinematic viscosity, m<sup>2</sup> s<sup>-1</sup>
- ξ mass fraction,
- σ surface tension, kg s<sup>-2</sup>

## Subscripts

- 1 liquid
- g1 small bubble fraction
- g2 large bubble fraction
- s solid

# Acknowledgements

The authors gratefully acknowledge the financial support of the German Research Foundation (DFG).

The calculations are performed using the IBM pSeries 690 super computer of the North German Supercomputing Combine (HLRN) in Hannover and Berlin.

#### References

- [1] Deckwer, W.-D. (1992). Bubble Column Reactors, John Wiley Sons, New York
- [2] Nigam, K.D.P., Schumpe, A. (1996). Three-phase sparge reactors. Gordon and Breach,

#### Amsterdam.

- [3] Lehr, F., Millies, M., Mewes, D. (2002). Bubble-size distributions and flow fields in bubble columns. AIChE J., 11, 2426-2443.
- [4] Wiemann, D. (2005), Numerisches Berechnen der Strömungs- und Konzentrationsfelder in n zwei- und dreiphasig betriebenen Blasensäulen, Thesis, Univ. of Hannover, Cuvillier-Verlag, Göttingen.
- [5] Wiemann, D., Mewes, D. (2005). Prediction of backmixing and mass transfer in ubble columns using a multifluid model. Ind. & Eng. Chem. Res., 44, 4959-4967.
- [6] Wiemann, D., Mewes, D. (2005). Calculation of flow fields in two- and three-phase bubble columns considering mass transfer. Chem. Eng. Sci., 60, 6085-6093.
- [7] Clift, R., Grace, J.R., Weber, M.E. (1978). Bubbles, Drops and Particles, Academic Press, New York, San Francisco, London.
- [8] Law, C.N.S., & Khoo, B.C. (2002). Transport across a turbulent air-water interface. AIChE J., 48, 1856-1868.
- [9] Lopez de Bertodano, M., Lahey, R.T., Jones, O.C. (1994). Development of a k-□ model for bubbly two-phase flow. J. Fluids. Eng., 1, 128-134.
- [10] C.K.K. Lun, F.B. Savage, D.J. Jeffrey, N. Chepurniy: Kinetic theories of granular flow and slighly inelastic particles in a general flow-field; J. Fluid Mech. 140 (1984), 223/256.
- [11] E. Santacesaria, M. Di Serio, A. Russo, U. Leone, R. Velotti: Kinetic and catalytic aspects in the hydrogen peroxide production via anthraquinone; Chem. Eng. Sci. 54 (1999), 13-14, 2799/2806.
- [12] H. Brauer: Particle/Fluid Transport processes; Progress in Chem. Eng. 17 (1979), 61/99.

